International Journal of Fatigue xxx (2008) xxx–xxx

Contents lists available at ScienceDirect

International Journal of Fatigue

journal homepage: www.elsevier.com/locate/ijfatigue

Thermomechanical fatigue evaluation and life prediction of 316L(N) stainless steel

A. Nagesha [a], M. Valsan [a], R. Kannan [a], K. Bhanu Sankara Rao [a,*], V. Bauer [b], H.-J. Christ [c], Vakil Singh [d]

[a] Mechanical Metallurgy Division, Indira Gandhi Centre for Atomic Research, Kalpakkam, Tamil Nadu 603 102, India
[b] Wieland-Werke Ag, 89079 Ulm, Germany
[c] Institut für Werkstofftechnik, Universität Siegen, D-57068 Siegen, Germany
[d] Centre of Advanced Study, Department of Metallurgical Engineering, Institute of Technology, Banaras Hindu University, Varanasi 221 005, India

ARTICLE INFO

Article history:
Received 4 July 2007
Accepted 16 March 2008
Available online xxxx

Keywords:
316L(N) stainless steel
Thermomechanical fatigue
In-phase
Out-of-phase
Life prediction

ABSTRACT

An attempt has been made to understand the thermomechanical fatigue (TMF) behaviour of a nitrogen-alloyed type 316L austenitic stainless steel under different temperature domains. Smooth, hollow specimens were subjected to in-phase (IP) and out-of-phase (OP) thermal–mechanical cycling in air under a mechanical strain control mode, at a strain rate of $6.4 \times 10^{-5}\ s^{-1}$ and a strain amplitude of ±0.4%. For the sake of comparison, total strain controlled low cycle fatigue (LCF) tests were also performed at the peak temperatures of TMF cycling on similar specimens employing the same strain rate and strain amplitude. Life was found to depend on the thermal/mechanical phasing and temperature. Creep was found to contribute to life reduction in IP tests when the peak temperature of cycling was above 600 °C. A few TMF tests were performed in vacuum in order to assess environmental influence on life. Thermomechanical fatigue cycling led to the development of significant amounts of mean stresses and the stress response was generally higher compared to that of LCF tests at the peak cyclic temperatures. Also, the isothermal tests at the peak temperature of TMF cycling resulted in lower lives compared to those obtained under TMF. An attempt was made to predict the TMF life using the isothermal database and satisfactory predictions were achieved using the Ostergren's frequency modified damage function (FMDF) approach.

1. Introduction

The heating and cooling cycles during startup and shutdown operations, such as those expected in high temperature industrial components, cause thermal stresses that often occur in combination with mechanical loads. The resulting thermomechanical fatigue (TMF) is often a life-limiting factor in these components and a widespread cause of failure. Traditionally, isothermal low cycle fatigue (LCF) tests have been used to assess the performance of materials subjected to TMF cycling. In most cases though, the deformation and damage under TMF cannot be predicted based on the data generated by isothermal testing since mechanical properties are typically temperature-dependent.

The two extreme and basic experimental TMF cycle types that are most often used to assess life under TMF conditions are in-phase (IP) TMF (peak tensile strain and peak temperature coinciding) and out-of-phase (OP) TMF (peak tensile strain and the minimum temperature coinciding). For a TMF cycle therefore, the hysteresis loops are "unbalanced" in tension vs. compression. In the OP-TMF case, considerably greater inelastic strain develops in compression in comparison with that under tension while the opposite holds true in the IP case.

Austenitic stainless steels are sensitive to thermal fatigue because of a low thermal conductivity combined with a high coefficient of thermal expansion. Extensive work has been reported in the literature on the TMF behaviour of different types of stainless steels. Fujino and Taira [1] demonstrated that for type 304 stainless steel cycled between 200 and 750 °C, the IP TMF lives were shorter than the lives in OP cycling by a factor of nearly four, while the isothermal fatigue lives at the peak temperature were seen to be in between the IP and OP lives. However, as the maximum temperature was lowered to 600 °C, the lives under IP, OP and peak temperature isothermal cycling were seen to converge. It was reported that the grain boundary sliding due to unbalanced displacements at the microlevel becomes pronounced as the peak temperature increased. Kuwabara and Nitta [2,3], working on the same material, reported that in the temperature range 300–600 °C, the IP lives were shorter than OP lives but isothermal lives at 600 °C yielded the lowest life. They also reported significant intergranular cracking in IP cycling compared to isothermal and OP cycling. Zauter et al. [4–6], through a systematic investigation on the TMF behaviour of 304L stainless steel in vacuum, reported that the TMF damage development and life were governed by the maximum temperature of cycling. They observed that when the peak cyclic temperature was below the creep range, IP and OP cycling resulted in similar lives and cracking was mostly transgranular. However, when the maximum temperature encompassed the

* Corresponding author. Tel.: +91 44 27480107; fax: +91 44 27480075.
E-mail address: bhanu@igcar.gov.in (K. Bhanu Sankara Rao).

0142-1123/$ - see front matter © 2008 Elsevier Ltd. All rights reserved.
doi:10.1016/j.ijfatigue.2008.03.019

creep range, a change in the fracture mode to intergranular was noticed and IP cycling proved more detrimental. Ellison and Al-Zamily, in their investigations on 316 SS [7,8] observed that IP cycling yielded lower life, which was substantiated by creep degradation and associated intergranular cracking. However, Shi et al. [9] have found that in the case of 316L SS, there is no significant difference between the IP and OP lives in the low temperature ranges (250–500 °C), whereas the IP cycling yielded almost four times greater life compared to OP in the temperature range of 250–650 °C. This was attributed to a tensile mean stress and a greater hysteresis energy absorbed in the OP cycling conditions [9]. Creep-induced intergranular cracking has been reported to degrade the cyclic life of 316L(N) stainless steel, when the maximum temperature of the thermal cycle falls in the creep range [10].

Under TMF conditions, the damage mechanisms prevalent in materials comprise of three major aspects, namely, fatigue, environmental (oxidation), and creep damage. These damage mechanisms may act independently or in combination depending on the type of materials and operating conditions, such as the maximum and minimum temperatures, the temperature range, the mechanical strain range and strain rate, the phasing of temperature and strain, the dwell time, or environmental factors. Due to these complexities, a well-accepted framework for the prediction of TMF life is yet to evolve and various approaches have been attempted, most of which are non-isothermal generalizations of isothermally derived models [11]. Development of models using the isothermal data for predicting the TMF life is of great significance for the designers. In view of the experimental complication associated with TMF, there have been several attempts at predicting the TMF lives, utilising the isothermal LCF database [12–17]. Ellison and Al-Zamily predicted the TMF lives of 316 SS and 1CrMoV steels using linear damage summation (LDS), ductility exhaustion and strain range partitioning (SRP) approaches [7,8]. The SRP method yielded satisfactory prediction, while the LDS approach was not very successful and often proved non-conservative. The ductility exhaustion model yielded a conservative, though less accurate life estimation for both the steels [8]. The SRP approach and its variants were applied successfully for predicting TMF lives of different materials [18,19]. Techniques such as the step-stress and loop inversion [19] have been employed for calculation of the creep strain for incorporating into the SRP model. Various versions of linear damage accumulation, wherein the fatigue, creep and oxidation damages are linearly summed to ascertain the total damage, have also been evaluated and successfully employed for TMF life prediction [17,20–24]. Empirical models that are generally based on a combination of parameters such as the applied strain range, plastic strain, dwell time etc. proposed by several investigators [25–28] have found varying degrees of success. More recently, crack growth approaches based on fracture mechanics have been attempted by several investigators [23,24,29–35]. In this paper, the TMF life prediction has been attempted, employing the Ostergren's hysteresis energy and Tomkins' crack growth approaches.

2. Experimental

316L(N) stainless steel employed in the present study, was subjected to a solutionising treatment at 1373 K for 1 h, which yielded an average (linear intercept) grain size of 75 μm. The chemical composition of the alloy in wt% was as follows: 0.021% C, 1.75% Mn, 12% Ni, 17% Cr, 2.4% Mo, 0.078% N, 0.002% S, 0.023% P and balance Fe. Both IP and OP TMF tests were carried out on hollow tubular samples (Fig. 1) using a constant mechanical strain amplitude ($\Delta\varepsilon_{mech}$) of ±0.4% and a fixed strain rate of 6.4×10^{-5} s^{-1}. A couple of tests were also conducted at $\Delta\varepsilon_{mech}$ of ±0.25 and ±0.6% in order to examine the strain amplitude effects. The tubular specimen design allows for higher heating and cooling rates while maintaining a high degree of waveform control and lowers the radial temperature gradients during thermal cycling [36]. Furthermore, the extended parallel section easily accommodates the induction heater work coils. Temperature intervals of 200, 250 and 300 °C were employed and tests were carried out in the range, 300–650 °C.

The machine used for the present investigation was a ±100 kN servohydraulic fatigue testing system which is capable of imposing independently programmable temperature and mechanical strain profiles onto the test specimen. The grips were water-cooled which served the additional purpose of specimen cooling. Three *K*-type thermocouples -two at the gauge extremities and one at the center – were spot-welded onto the specimen surface. The thermocouple welded in the top of the gauge length was chosen as the controlling thermocouple, so as to keep the gradients to a minimum [36], while the other two served to monitor the temperatures along the rest of the gauge length. The spot welding process was optimized in order to avoid damage initiation at the thermocouple locations. The induction coil was adapted to the specimen geometry; it consisted of three independent segments that could be adjusted along the radial and vertical directions to ensure uniformity of temperature distribution in the test section. Strain was measured via an air-cooled, side-contacting extensometer that had a gauge length of 25 mm and a maximum strain capability of −5% to +10%.

The specimen was initially allowed to expand under zero load during initial heating from the ambient to peak temperature (650 °C). Subsequently, three thermal cycles were introduced between 300 and 650 °C, allowing for free thermal expansion and contraction under load control. The thermal strain, ε^{th} as a function of temperature was plotted and approximated by a polynomial of 2nd order. The mechanical strain from the relationship, $\varepsilon^{m} = \varepsilon^{t} - \varepsilon^{th}$ (where ε^{m} and ε^{t} represent the mechanical and total strains respectively) was calculated and controlled on a real-time basis. The TMF test results were compared with those obtained from isothermal LCF tests, which were carried out in the temperature range, 525–650 °C at a mechanical strain amplitude of ±0.4%. A few TMF tests were also performed in vacuum at a strain amplitude of ±0.6% in order to isolate the environmental influence on the cyclic life. With a view to having a meaningful comparison of the results, the samples used in LCF and TMF tests were of identical geometry. Further,

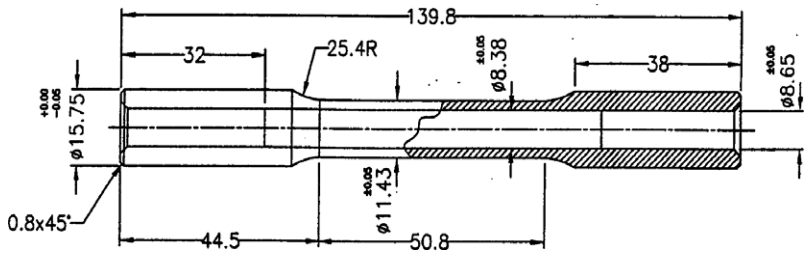

Fig. 1. Geometry of the test specimen (Dimensions in mm).

Please cite this article in press as: Nagesha A et al., Thermomechanical fatigue evaluation and life prediction of 316L(N) stainless steel, Int J Fatigue (2008), doi:10.1016/j.ijfatigue.2008.03.019

both the TMF and LCF tests were performed at the same strain rate ($6.4 \times 10^{-5}\ s^{-1}$), employing a triangular strain–time–temperature waveform. A 20% drop in tensile stress from the saturated value was used as the failure criterion in all the tests but a few tests were run upto the actual specimen separation.

3. Results and discussion

The cyclic stress response of the materials under both LCF and TMF conditions displayed in general, an initial hardening regime for the first 70–100 cycles followed by a well-defined saturation period that continued till the onset of crack initiation (Figs. 2–4). Fig. 3 provides a comparative stress response plot pertaining to IP and OP tests under three different temperature intervals (300–550, 350–600 and 400–650 °C). The influence of temperature range on the stress response is brought out in Fig. 4, wherein data from IP tests are plotted for different temperature intervals in the range, 350–650 °C. Fig. 5 illustrates the relationship between the stress responses obtained in TMF and peak temperature LCF tests. Saturation values of the peak stresses are plotted against the temperature

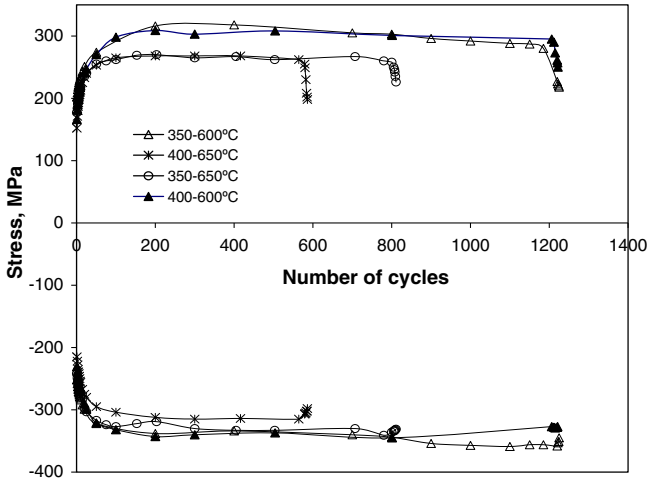

Fig. 4. Influence of temperature range on the stress response, in-phase cycling.

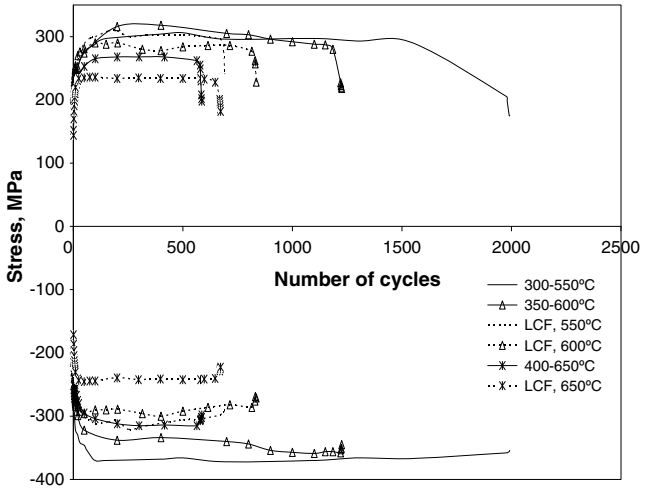

Fig. 2. Cyclic stress response obtained under in-phase TMF and isothermal LCF cycling, $\Delta\varepsilon_{mech} = \pm 0.4\%$.

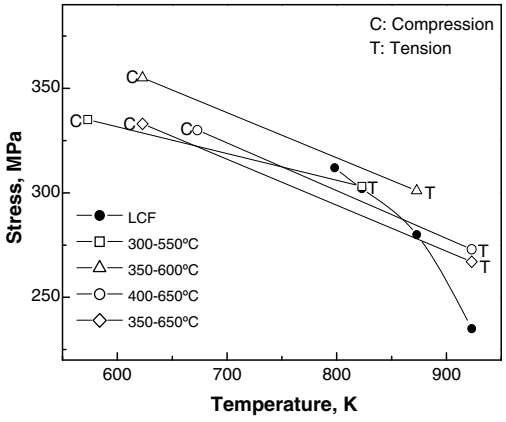

Fig. 5. Comparison of stress amplitudes in in-phase TMF and isothermal tests plotted against temperature.

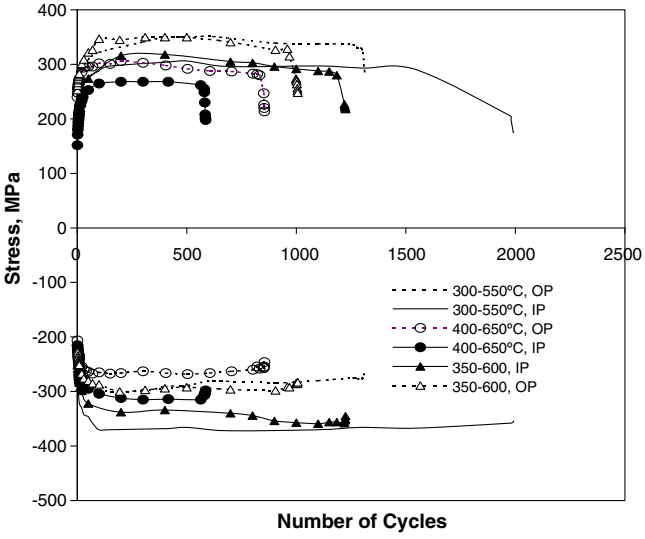

Fig. 3. Comparative cyclic stress response behaviour under in-phase and out-of-phase cycling.

using the absolute values of the stress, points marked C and T in the plot denoting compression and tension, respectively.

As can be seen from Fig. 2, the TMF cycling yielded a consistently higher stress response in comparison with LCF cycling at the peak temperature employed in TMF. This behaviour, also reflected in the saturation stress plot shown in Fig. 5, could be attributed to the higher flow stress of the material in the low temperature regimes of the TMF cycle. The observed stress response behaviour is typical of the solution-annealed alloy under strain controlled isothermal cycling conditions [37–40], and is seen to be strongly influenced by the mean temperature of cycling, as can be observed from Fig. 2. Stress data pertaining to a constant temperature interval of 250 °C are presented in the figure and the response stress was seen to shift downward as the mean temperature of the TMF cycle increased. In contrast to strain controlled isothermal LCF, the TMF cycling resulted in a mean stress, which is compressive under IP and tensile under OP cycling conditions, as shown in Fig. 3 and Table 1.

The TMF life was seen to decrease with increasing peak and mean temperatures of thermal cycling. It was noticed that TMF life in out-of-phase cycling is lower than that in the in-phase tests when the maximum temperature of TMF cycling (T_{max}) was less than or equal to 600 °C, while in the creep temperature domain ($T_{max} = 650$ °C), the IP tests yielded lower lives (Fig. 3 and Table 1). The lower life of the alloy in the OP testing conditions in the

Please cite this article in press as: Nagesha A et al., Thermomechanical fatigue evaluation and life prediction of 316L(N) stainless steel, Int J Fatigue (2008), doi:10.1016/j.ijfatigue.2008.03.019

Table 1
Summary of TMF and isothermal test results

ΔT (°C)	$\Delta\varepsilon_{mech}$ (%)	IP/OP	σ_{mean} (MPa)	TMF life	Isothermal life at T_{max}
300–550	±0.4	IP	−46	2093	693
		OP	+31	1312	
350–600	±0.4	IP	−27	1210	835
		OP	+30	1000	
400–650	±0.4	IP	−22	873	672
		OP	+15	853	
350–650	±0.4	IP	−34	811	672
		OP	+16	1256	
400–600	±0.4	IP	−15	1221	835
		OP	+17	709	
400–650	±0.25	IP	−9	2034	–
		OP	+16	3485	
400–650	±0.6	OP	+10	472	–
400–650[a]	±0.6	IP	−17	750	–
		OP	+13	3000	

[a] Tested in vacuum.

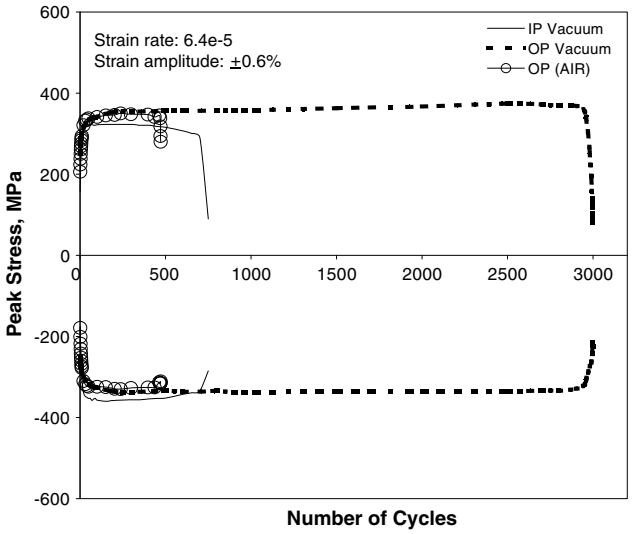

Fig. 6. Comparative cyclic stress response behaviour under in-phase and out-of-phase cycling in air and vacuum.

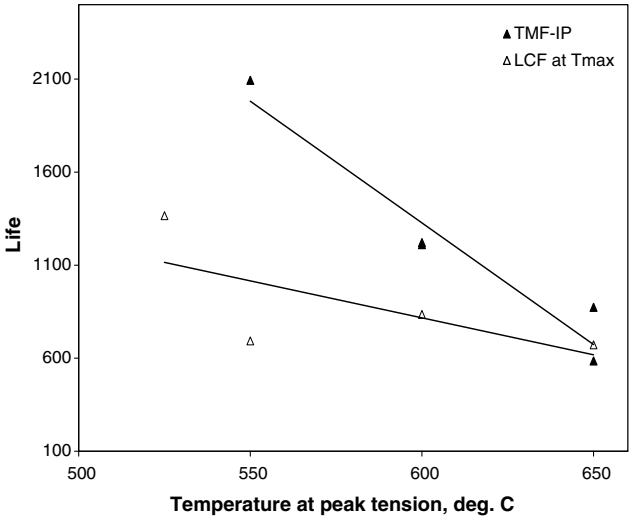

Fig. 7. Variation of TMF and isothermal LCF lives at T_{max} with the maximum cyclic temperature.

lower temperature regimes could be attributed to the development of a tensile mean stress and the higher stress level (Fig. 3) leading to an earlier crack initiation and a faster propagation. However, under conditions wherein the T_{max} was 650 °C, creep effects became pronounced and rendered IP cycling more damaging in comparison to OP cycling. Fatigue life variation with temperature range is illustrated in Fig. 4. It may be seen that with the minimum temperature (T_{min}) fixed at 350 °C, an upward shift of the T_{max} led to a reduction in life and a decrease in the response stress. Also, for a fixed T_{max} of 650 °C, an increase in the T_{min} resulted in life reduction though the response stress remains unaffected. The life reduction did not reflect in the response stress since the maximum temperature was identical and the tensile part of the cyclic stress response corresponds to the flow stress at T_{max}. Besides, the difference in the minimum temperature is only 50 °C in the two cases that are shown in the Fig. 4. Similarly, it may also be noted that the compressive response stresses were identical for the 350–600 °C and 350–650 °C IP cycling. It is pertinent to note here that the stress response is a representative of the general flow or deformation characteristics of the material rather than the fracture behaviour, which reflects through a rapid stress drop towards the end of life. Influence of creep on the TMF damage was evident in the form of extensive intergranular cracking in the 400–650 °C IP test. The isothermal tests conducted concurrently at the peak temperatures employed in the TMF cycles displayed lower lives compared to both the IP and OP tests (Table 1). Fig. 6 depicts the comparative stress response between tests conducted in air and vacuum at a strain amplitude of ±0.6%, with a temperature range of 400–650 °C. The role of environment on life could be clearly seen, with a 6-fold increase in life under vacuum, in comparison with that obtained in air. Fig. 7 shows a comparative plot of the cyclic lives obtained in IP TMF and isothermal LCF cycling at T_{max}. TMF lives obtained at a constant temperature interval of 250 °C have been used for the comparison. The progressive reduction in the difference between the TMF and peak temperature LCF lives seen in the figure could be a consequence of the damaging influence of dynamic strain ageing (DSA) that operates when the temperature range of TMF cycling encompasses the DSA domain. Thermomechanical cycling proves to be particularly detrimental under conditions wherein the minimum and maximum temperatures of cycling lie, respectively below and above the temperature range, where DSA is active [4]. In the 400–650 °C IP test, DSA plays a significant role in failure in this steel whereas in the isothermal test at 650 °C, there is no influence of DSA. The temperature range for the occurrence of DSA in this alloy has been established to be between 500 and 600 °C [39,40]. However, depending on the applied strain rate, DSA has been found to manifest between 250 and 650 °C in a similar material with the lower strain rates decreasing the upper temperature limit for the operation of DSA [41]. At a lower strain rate of 1×10^{-4} s^{-1}, it has been reported in the temperature range of 250–550 °C. The saturated stress amplitude plotted against test temperature obtained from the isothermal tests and presented in Fig. 8 shows a near plateau region between 550 and 600 °C, which could be associated with DSA. Hence, the influence of DSA would be felt more in the case of IP cycling between 400 and 650 °C in comparison to isothermal LCF at 650 °C, thereby bringing down the TMF life. In the temperature range of 400–650 °C, IP cycling yielded lower life than OP cycling in both air and vacuum environments. The above differences in cyclic lives can be attributed to a combined influence of oxidation and creep in IP tests under air environment and to pure creep under IP-vacuum. Whereas oxidation and creep contribute to life reduction under isothermal cycling at 650 °C, a combined influence of oxidation, creep and DSA results in a more drastic life reduction in the 400–650 °C IP test. Metallographic examination of the longitudinally cut sections on the sample surface revealed that the crack initiation and propaga-

Please cite this article in press as: Nagesha A et al., Thermomechanical fatigue evaluation and life prediction of 316L(N) stainless steel, Int J Fatigue (2008), doi:10.1016/j.ijfatigue.2008.03.019

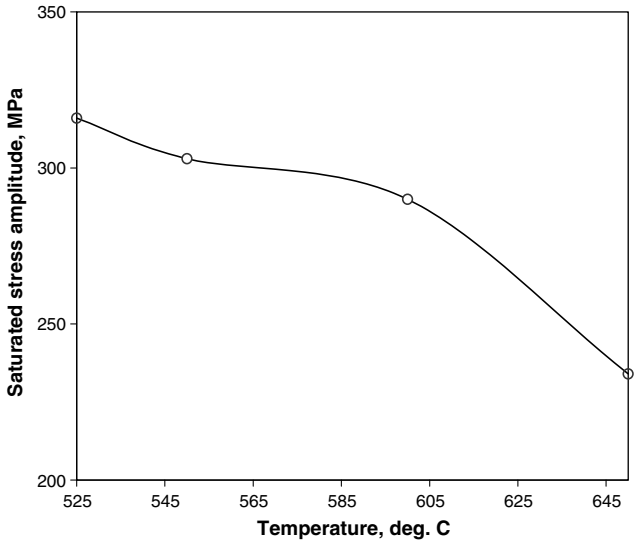

Fig. 8. Dependence of saturated stress amplitude on temperature in isothermal tests.

tion occurred in a transgranular mode under both OP and IP cycling conditions (with $T_{max} \leqslant 600$ °C for the latter case), Fig. 9a–c. However, in cases where the T_{max} was 650 °C, IP cycling proved to be more deleterious as a consequence of a creep-dominated intergranular cracking that was seen to be aided by oxidation, Fig. 10a and b. The compressive mean stress in this case does not result in an enhancement in the TMF life since the damaging influence imparted by creep eclipses the beneficial effect of the mean stress. This behaviour is consistent with a reported observation on austenitic type 304 stainless steel [4], wherein it was shown that a creep-dominant failure is expected to occur in TMF cycling if the T_{max} exceeds the creep temperature (T_{cr}) such that $(T_{max} - T_{cr})/\Delta T$ remains above 5%, ΔT being the difference between T_{max} and T_{min}. Influence of oxidation was more prominent in the IP tests as a consequence of the cracks remaining open at the high temperature end of the TMF cycle, thereby allowing easy environmental access to the crack tips. Evidence of creep-dominated intergranular cracking was clearly seen on the fracture surface of specimen tested under 400–650 °C IP cycling. Fig. 10c shows creep-induced intergranular cracking interspersed with clear striations under the above testing condition. Fig. 10d presents a fractograph showing a predominantly intergranular failure with clear grain boundary facets in the sample tested in vacuum at 400–650 °C IP cycling with a strain amplitude of ±0.6%.

4. Life prediction under TMF cycling

In order to design components operating under TMF cycling conditions, reasonably accurate estimation of the fatigue life has to be made. Since, it is not always possible to carry out a large number of TMF experiments (which are both complicated and expensive) to obtain enough data, TMF life prediction using isothermal database becomes handy. In this section, it is attempted to compare the experimental TMF lives with those predicted using data generated from both isothermal and TMF tests, using the frequency modified damage function and Tomkins' crack growth approaches.

4.1. Frequency modified damage function

Since, the fatigue damage is generally caused by the cyclic plastic strain, the plastic strain energy plays an important role in the damage process. Therefore, the idea of correlating the fatigue life with the plastic work during strain cycling has gained much attention [17,42–53]. Fatigue damage is primarily controlled by the

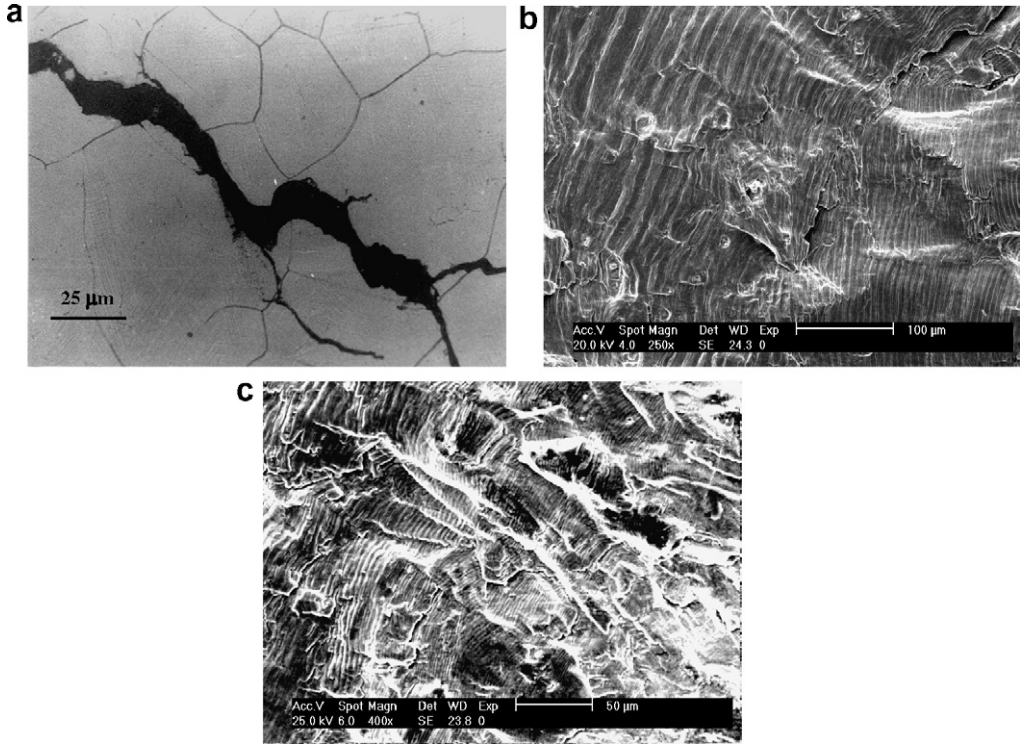

Fig. 9. (a) and (b): Optical metallograph and SEM fractograph respectively, showing transgranular cracking under 300–550 °C in-phase cycling and (c) SEM fractograph showing transgranular stage-2 crack growth in 400–650 °C out-of-phase cycling.

Please cite this article in press as: Nagesha A et al., Thermomechanical fatigue evaluation and life prediction of 316L(N) stainless steel, Int J Fatigue (2008), doi:10.1016/j.ijfatigue.2008.03.019

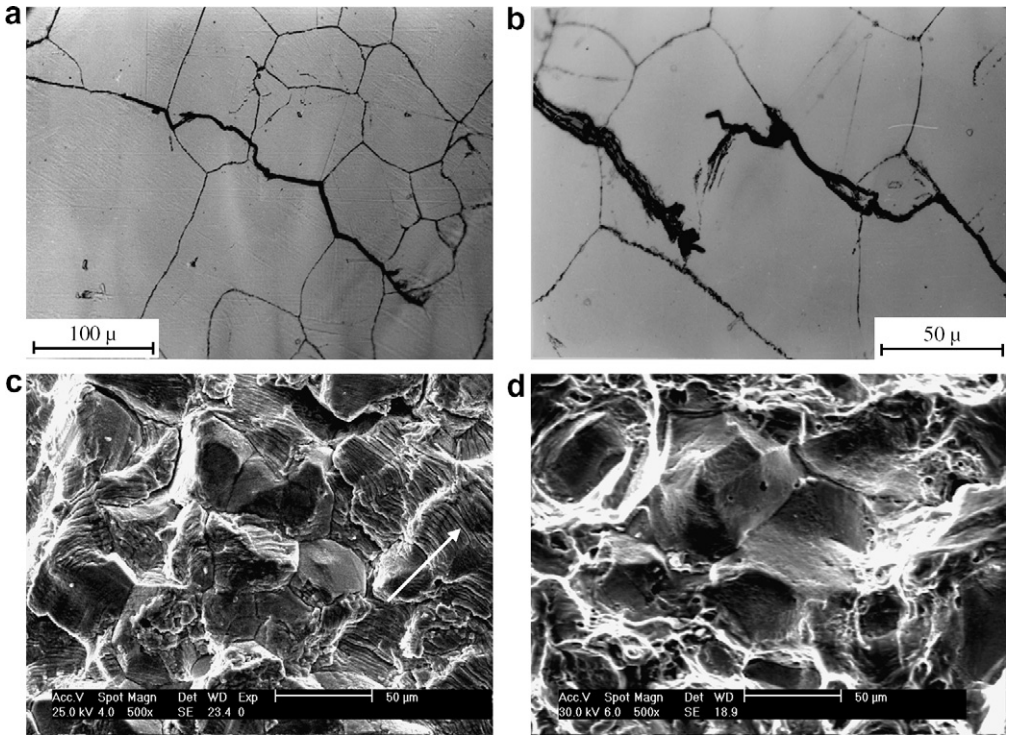

Fig. 10. (a) Mixed mode cracking assisted by oxidation, (b) and (c) SEM fractograph showing creep-dominated intergranular cracking interspersed with clearly defined striations (pointed by the arrow) in 400–650 °C in-phase cycling and (d) fractograph showing clear grain boundary facets in sample tested under vacuum at 400–650 °C in-phase cycling (tensile axis is vertical and the arrow in (c) indicates the average crack growth direction).

stress and plastic strain or the irrecoverable plastic strain energy per cycle. Usually, the hysteresis loop at half-life is taken to be a representative one and is used to calculate the plastic strain energy. Ostergren [43] proposed a damage function that includes stress as well as strain range, to describe failure. The basic assumption of the method is that the net tensile hysteresis energy is a measure of damage and can be approximated by $\sigma_T \Delta\varepsilon_p$, where σ_T and $\Delta\varepsilon_p$ are the half-life values of the peak tensile stress and plastic strain amplitude respectively. This energy term has been seen to have a direct correlation with the cyclic life of materials in isothermal LCF [43,51] and TMF cycling conditions [17,27,50,53–55].

The cyclic life could be related to the plastic strain energy by a power law relationship [43],

$$N_f = L \times (\sigma_{max} \times \Delta\varepsilon_p)^{\eta}$$

where η and L are material parameters which could be determined from isothermal LCF tests. σ_{max} and $\Delta\varepsilon_p$ are the half-life values of the peak tensile stress and plastic strain amplitude, respectively. The above equation could be modified in order to account for time-dependent processes during non-isothermal cycling [50] as,

$$N_f = L \times (\sigma_{max} \times \Delta\varepsilon_p)^{\eta} \times (v^*)^{(1-k)}$$

where k is another constant and v^* is the effective frequency, which was calculated as, $v^* = 1/(\tau + \Delta\tau)$. Where τ is the cycle time and $\Delta\tau$ is the time per cycle during which creep occurs [50]. It may be noted that the hysteresis loop asymmetry in the IP and OP cycling would lead to different lifetimes because of the presence of the σ_{max} term in the life equation. Data pertaining to continuous cycling low cycle fatigue under different frequencies were utilized for deriving the parameters in the above damage equation. The parameters L, η and k were computed using the isothermal low cycle fatigue data from National Institute for Materials Science, Japan [56] for 316 SS in the temperature range, 500–700 °C since the LCF lives of 316 SS and 316L(N) SS are reported to be comparable [57]. Multiple regression analysis yielded values of 2553, −1.53 and 0.808 for L, η and k, respectively. Subsequently, these damage parameters were utilized for predicting TMF life of 316L(N) SS in the temperature range, 300–650 °C. A satisfactory prediction, within a scatter band factor of two could be obtained as shown in Fig. 11.

4.2. Tomkins' crack growth model

The concept of using cyclic crack tip displacements to characterise the crack growth rate behaviour has been applied for many

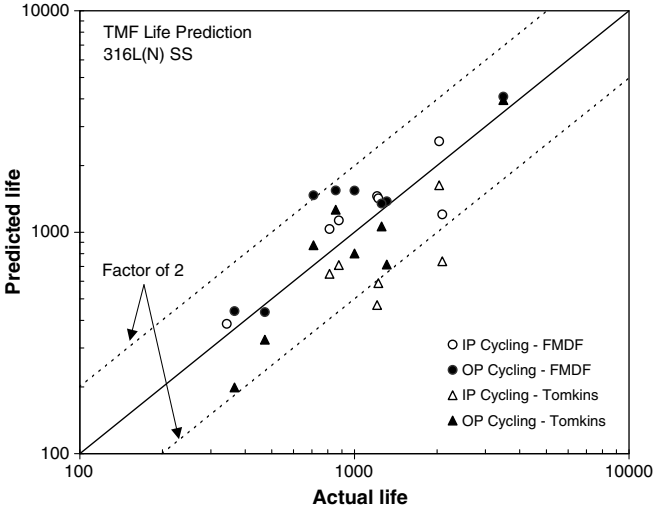

Fig. 11. Comparison between the experimental and calculated TMF lives using the FMDF and Tomkins' crack growth approach approaches. Prediction within a factor of two is largely achived.

Please cite this article in press as: Nagesha A et al., Thermomechanical fatigue evaluation and life prediction of 316L(N) stainless steel, Int J Fatigue (2008), doi:10.1016/j.ijfatigue.2008.03.019

years [58,59]. Herein, it is thought that the cyclic crack tip displacement is a more fundamental parameter to characterise the crack tip damage. The Tomkins' model [59] assumes that under conditions of high strain cycling, the time spent in the crack initiation stage is small and the damage occurs on a 45° shear plane at the crack tip during the tensile half of each cycle. The model permits calculation of the amount of cyclic crack growth, an integration of which yields the fatigue endurance. The crack growth equation is written as follows:

$$\frac{da}{dN} = Ba$$

where [60]

$$B = \Delta\varepsilon_p \left[\frac{1}{\cos\left[\frac{\pi}{2} \cdot \frac{\sigma}{R_m}\right]} - 1 \right]$$

The above is an empirical equivalent of the equation proposed by Tomkins [59]. In the above equation, σ and R_m are, respectively, the maximum response stress and the UTS at the temperature where peak tensile strain occurs. The fatigue life can be obtained from an integration of the crack growth equation. An initial crack length of 75 μm (grain size of the material) was used for the prediction. The fatigue cracks, on an average, propagated to a length of 1.2 mm and hence a final crack length of 1.2 mm was assumed. A conservative life prediction, largely within a scatter band of two could be obtained, as shown in Fig. 11.

5. Conclusions

Thermomechanical fatigue behaviour of 316L(N) stainless steel was evaluated under different temperature regimes using IP and OP cycling. Creep and oxidation were seen to play a significant role in the damage under IP cycling when the peak temperature of TMF cycling encompassed the creep range. Isothermal cycling at the peak temperature of TMF yielded lower lives compared to both IP and OP cycling. However, the difference in life between the isothermal and TMF lives were seen to diminish with increase in the peak temperature of TMF cycling. Testing under vacuum resulted in a six-fold increase in life under OP cycling, underlining a strong environmental influence on life. Ostergren's frequency modified damage function approach was successfully employed for predicting the TMF life, utilising the isothermal database. Tomkins' crack growth model yielded a conservative prediction, largely within a factor of two. The investigation showed that the practice of high temperature component design for low cycle fatigue based on the expected peak operative temperature is generally conservative for the present material.

Acknowledgements

The authors wish to acknowledge Dr. Baldev Raj, Director, IGCAR for his constant encouragement and support. Financial assistance by DST and DAAD under the project, INT/DAAD/P-38/2001, towards the work is gratefully acknowledged.

References

[1] Fujino M, Taira S. Effect of thermal cycling on low cycle fatigue life of steels and grain boundary sliding characteristics. Proc ICM 3 1979;2:49–58.
[2] Kuwabara K, Nitta A. Thermal–mechanical low cycle fatigue under creep–fatigue interaction on type 304 stainless steel. Proc ICM 3 1979;2:69–78.
[3] Kuwabara K, Nitta A. Effect of strain hold time of high temperature on thermal fatigue of type 304 stainless steel. ASME-MPC symposium on creep–fatigue interaction. American Society of Mechanical Engineers; 1976. p. 161–77.
[4] Zauter R, Christ H-J, Mughrabi H. Fatigue damage. Met Mater Trans 1994;25A:401–6.
[5] Zauter R, Christ H-J, Mughrabi H. Some aspects of thermomechanical fatigue of AISI 304L stainless steel: part II. Dislocation arrangements. Met Mater Trans 1994;25A:407–13.
[6] Zauter R, Petry F, Christ H-J, Mughrabi H. Thermomechanical fatigue behaviour of materials. In: Sehitoglu H, editor. ASTM STP 1186. Philadelphia: American Society for Testing and Materials; 1993. p. 70–90.
[7] Ellison EG, Al-Zamily A. Stress response under thermal mechanical strain cycling for a 1 Cr–Mo–V ferritic steel and two 316 stainless steels. Fatigue Fract Eng Mater Struct 1994;17(1):39–51.
[8] Ellison EG, Al-Zamily A. Fracture and life prediction under thermal–mechanical strain cycling. Fatigue Fract Eng Mater Struct 1994;17(1):53–67.
[9] Shi HJ, Wang ZG, Su HH. Thermomechanical fatigue of a 316L austenitic steel at two different temperature intervals. Scripta Mat 1996;35(9):1107–13.
[10] Nagesha A, Valsan M, Bhanu Sankara Rao K, Kannan R, Mannan SL. Thermomechanical fatigue behaviour of type 316L(N) austenitic stainless steel. Trans IIM 2005;58(2–3):373–8.
[11] Cai C, Liaw PK, Ye M, Yu J. Recent developments in the thermomechanical fatigue life prediction of superalloys. J Met-e 1999;51(4).
[12] Taira S. Relationship between thermal fatigue and low cycle fatigue at elevated-temperature. ASTM STP 520 1973:80–101.
[13] Taira S, Motoaki F, Takashi H. A method for life prediction of thermal fatigue by isothermal fatigue testing. Symp Mech Behav Mater: Soc Mater Sci, Kyoto 1974:257–64.
[14] Shi H, Robin C, Pluvinage G. Thermal–mechanical fatigue lifetime prediction of an austenitic stainless steel. ASTM STP1211 1993:105–16.
[15] Nitta A, Kuwabara K. Thermal–mechanical fatigue failure and life prediction. High temperature creep–fatigue, vol. 3. Elsevier Applied Science, Current Japanese Materials Research, Elsevier; 1988.
[16] Degallaix G, Corn C, Pluvinage G. Lifetime prediction on Cr–Mo–V and 316L steels under thermal and mechanical cycling. Fatigue Fract Eng Mater Struct 1990;13(5):473–85.
[17] Christ HJ, Maier H-J, Teteruk R. Thermomechanical fatigue behaviour of metallic high temperature materials. Trans Indian Inst Met 2005;58(2–3):197–205.
[18] Halford GR, Manson SS. Life prediction of thermal–mechanical fatigue using strain range partitioning. ASTM STP 612 1976:239–54.
[19] Nitta A, Kuwabara K, Kitamura T. Prediction of thermal fatigue life in high temperature component materials for power plant. CRIEPI report E282015; 1983.
[20] Sehitoglu H. Thermomechanical fatigue life prediction methods, advances in fatigue lifetime predictive techniques. Oxidation and creep: part 2 – life prediction. ASTM STP 1122 1992:47–76.
[21] Neu RW, Sehitoglu H. Thermomechanical fatigue, oxidation and creep: part 2 – life prediction. Met Trans A 1989;20A:1769–83.
[22] Sehitoglu H, Boismier DA. Thermomechanical fatigue of Mar-M247: part 2 – life prediction. J Eng Mat Tech 1990;112:80–9.
[23] Christ H-J, Jung A, Maier HJ, Teteruk R. Thermomechanical fatigue – damage mechanisms and mechanism-based life prediction methods. SADHANA 2003;28(1–2):147–65.
[24] Maier HJ, Teteruk RG, Christ H-J. Modeling thermomechanical fatigue life of high temperature titanium alloy IMI 834. Met Mater Trans 2000;31A:431–44.
[25] Woodford DA, Mowbray DF. Effects of materials characteristics and test variables on thermal fatigue of cast superalloys. Mater Sci Eng 1974;16:5–43.
[26] Bernstein HL, Grant TS, McClung RC, Allen JM. Prediction of thermal–mechanical fatigue life for gas turbine blades in electric power generation. Thermomechanical fatigue behaviour of materials. ASTM STP 1186 1993:212–38.
[27] Zamrik SY, Davis DC, Firth LC. Isothermal and thermomechanical fatigue of type 316 stainless steels. Thermomechanical fatigue behaviour of materials. ASTM STP 1263 1996:96–116.
[28] Kanasaki H, Hirano A, Iida K, Asada Y. Corrosion fatigue behaviour and life prediction method under changing temperature conditions. Effects of the environment on the initiation of crack growth. ASTM STP 1298 1997: 267–81.
[29] Okazaki M, Koizumi T. Crack propagation during low cycle thermal–mechanical and isothermal fatigue at elevated-temperatures. Metall Trans 1983;14A:1641–8.
[30] Jordan EH, Meyers GJ. Fracture mechanics applied to non-isothermal fatigue crack growth. Eng Fract Mech 1986;23:345–58.
[31] Miller MP, McDowell DL, Oehmke RLT, Antolovich SD. A life prediction model for thermomechanical fatigue based on microcrack propagation. ASTM STP1186 1993:35–49.
[32] Dai J, Marchand NJ, Hongoh M. Thermal mechanical fatigue crack growth in titanium alloys: experiments and modeling. ASTM STP1263 1996:187–209.
[33] Kadioglu Y, Sehitoglu H. Thermomechanical and isothermal fatigue behaviour of bar and coated superalloys. J Eng Mater Technol 1996;118:94–102.
[34] Bauer V, Christ H-J. Application of a fracture mechanics concept to life prediction of austenitic stainless steels under TMF loading conditions. Trans Indian Inst Met 2005;58(2–3):475–80.
[35] Nissley DM. Thermomechanical fatigue life prediction in gas turbine superalloys – a fracture mechanics approach. AIAA J 1995;33(6):1114–20.
[36] Castelli MG, Ellis JR. Improved techniques for thermomechanical testing in support of deformation modeling. In: Sehitoglu H, editor. Thermomechanical fatigue behaviour of materials ASTM STP 1186. Philadelphia: American Society for Testing and Materials; 1993. p. 195–211.
[37] Nilsson J-O. Fatigue Fract Eng Mater Struct 1984;7(1):55.

Please cite this article in press as: Nagesha A et al., Thermomechanical fatigue evaluation and life prediction of 316L(N) stainless steel, Int J Fatigue (2008), doi:10.1016/j.ijfatigue.2008.03.019

[38] Degallaix S, Degallaix G, Foct J. In: Solomon HD, Halford GR, Kaisand LR, Leis BN, editors. Low cycle fatigue ASTM STP 942. Philadelphia: American Society for Testing and Materials; 1988. p. 798.
[39] Srinivasan VS, Sandhya R, Bhanu Sankara Rao K, Mannan SL, Raghavan KS. Effect of temperature on the low cycle fatigue behaviour of nitrogen alloyed type 316L stainless steel. Int J Fatigue 1991;13(6):471–8.
[40] Srinivasan VS, Sandhya R, Valsan M, Bhanu Sankara Rao K, Mannan SL. The influence of dynamic strain ageing on stress response and fatigue life of 316L(N) stainless steel. Scripta Mater 1997;37:1593–8.
[41] Hong S-G, Lee K-O, Lee S-B. Dynamic strain aging effect on the fatigue resistance of type 316L stainless steel. Int J Fatigue 2005;27:1420–4.
[42] Halford GR. The energy required for fatigue. J Mater 1966;1:3–18.
[43] Ostergren WJ. A damage function and associated failure equations for predicting hold time and frequency effects in elevated-temperature low cycle fatigue. J Test Eval 1976;4(5):327–39.
[44] Santner JS, Fine ME. The hysteretic plastic work as a failure criterion in a Coffin–Manson type relation. Scripta Metall 1977;11(2):159–62.
[45] Lefebvre D, Ellyin F. Cyclic response and inelastic strain energy in low cycle fatigue. Int J Fatigue 1984;6(1):9–15.
[46] Kliman V. Fatigue life estimation under random loading using the energy criterion. Int J Fatigue 1985;7:39–44.
[47] Golos K, Ellyin F. A total strain energy density for cumulative fatigue damage. ASME J PVT 1988;6:36–41.
[48] Skelton RP. Energy criterion for high temperature low cycle fatigue. Mater Sci Tech 1991;7:427–39.
[49] Bily M. Cyclic deformation and fatigue of metals. Amsterdam: Elsevier Publisher; 1993.
[50] Maier HJ, Teteruk R, Christ H-J. Modelling thermomechanical fatigue life. Mater High Temp 2002;19(1):9–17.
[51] Ellyin F, Kujawski D. Plastic strain energy in fatigue failure. ASME J Press Vess Tech 1984;106:342–7.
[52] Radhakrishnan VM. An analysis of low cycle fatigue based on hysteresis energy. Fatigue Fract Eng Mater Struct 1980;3(1):75–84.
[53] Liu F, Ai SH, Wang YC, Zhang H, Wang ZG. Thermal–mechanical fatigue behaviour of a cast K417 nickel-based superalloy. Int J Fatigue 2002;24:841–6.
[54] Shi HJ, Pluvinage G. Cyclic stress–strain response during isothermal and thermomechanical fatigue. Int J Fatigue 1994;16(8):549–57.
[55] Radhakrishnan VM. An energy based analysis of thermomechanical fatigue. Trans Indian Inst Met 1996;49(4):357–69.
[56] Data sheets on elevated-temperature high-cycle and low cycle fatigue properties of SUS316-HP (18Cr–12Ni–2Mo) hot rolled stainless steel plate, NRIM/FDS/No. 15; 1979.
[57] Srinivasan VS, Valsan M, Sandhya R, Kannan R, Bhanu Sankara Rao K, Mannan SL. In: Proceedings of the seminar on materials R&D for PFBR, Kalpakkam: IGCAR; January 1–2, 2003. p. 77.
[58] Weertman J. Rate of growth of fatigue cracks calculated from the theory of infinitesimal dislocations distributed on a crack plane. Int J Fract 1966;2:460–7.
[59] Tomikns B. Fatigue crack propagation – an analysis. Phil Mag 1968;18: 1041–66.
[60] Remy L. Fatigue and thermomechanical fatigue at high temperature. In: Jurgan Buschow KH, Cahn Robert W, Flemings Merton C, Ilschner Bernard, Kramer Edward J, Mahajan Subhash, editors. Encyclopedia of materials: science and technology, vol. 3. Elsevier Science; 2001. p. 2868–79.

Please cite this article in press as: Nagesha A et al., Thermomechanical fatigue evaluation and life prediction of 316L(N) stainless steel, Int J Fatigue (2008), doi:10.1016/j.ijfatigue.2008.03.019